

1 Supporting information for ‘Complexity in Biogeochemical 2 Models: Consequences for the Biological Carbon Pump’

3
4 Jonathan Rogerson^{1*}, Alessandro Tagliabue², Agathe Nguyen¹, Marcello Vichi^{3,4}, Lewis Wrightson²,
5 Prima Anugerahanti^{2,5}, Olivier Aumont⁶ & Marion Gehlen¹

6
7 ¹Laboratoire des Sciences du Climat et de l'Environnement, LSCE/IPSL, CEA-CNRS-UVSQ, Université Paris-Saclay,
8 Gif-sur-Yvette, FR. ²Department of Earth Ocean, and Ecological Sciences, School of Environmental Sciences,
9 University of Liverpool, Liverpool, UK. ³Department of Oceanography, University of Cape Town, Cape Town, RSA.
10 ⁴Marine and Antarctic Research centre for the Innovation and Sustainability (MARIS), Cape Town, RSA. ⁵National
11 Oceanography Centre, Liverpool, UK. ⁶Sorbonne Université, CNRS/IRD/MNHN, LOCEAN-IPSL, Paris, FR.

12
13 *Corresponding author: Jonathan Rogerson: jonathan.rogerson@lsce.ipsl.fr

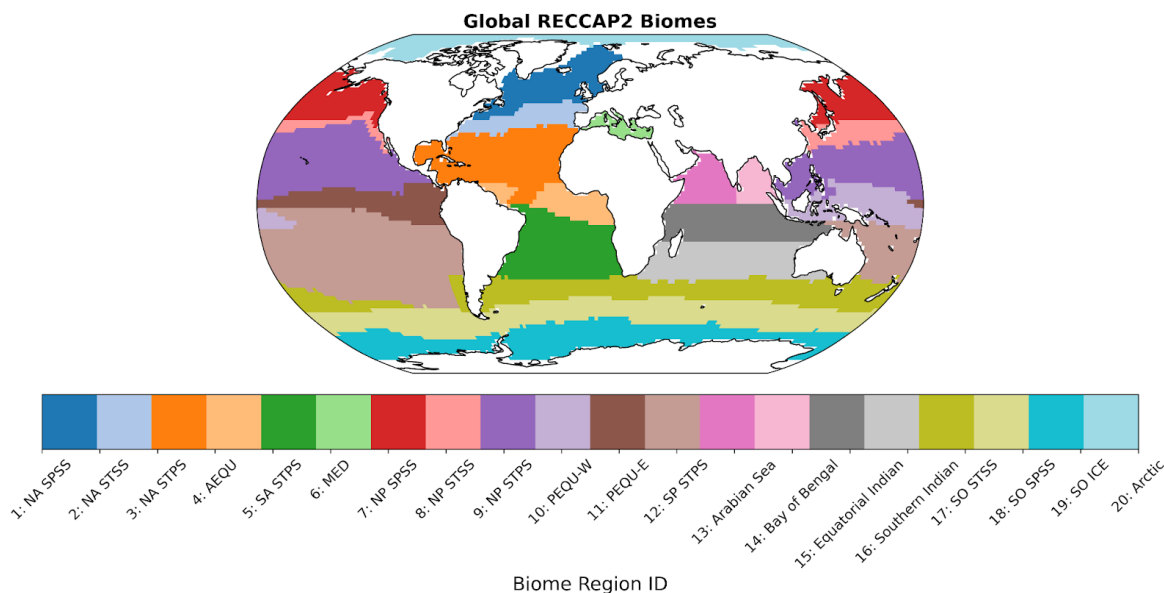
14 15 Introduction

16
17 This supplementary section provides additional details and supporting analyses related to the main
18 manuscript. It includes the following:

19
20 **S1** - Regional Carbon Cycle Assessment and Processes (RECCAP2) biomes
21 **S2** - Different remote-sensing NPP algorithms
22 **S3** - Different remote-sensing export production algorithms
23 **S4** - Export production equations and references
24 **S5** - Ensemble mean NPP and C_{exp} of PISCES and remote-sensing
25 **S6** - Phytoplankton biomass percentage contribution in Quota-based configurations
26 **S7** - Zooplankton dynamics
27 **S8** - Skill assessment of PISCES configurations versus ensemble mean of remote-sensing
28 NPP and C_{exp} .

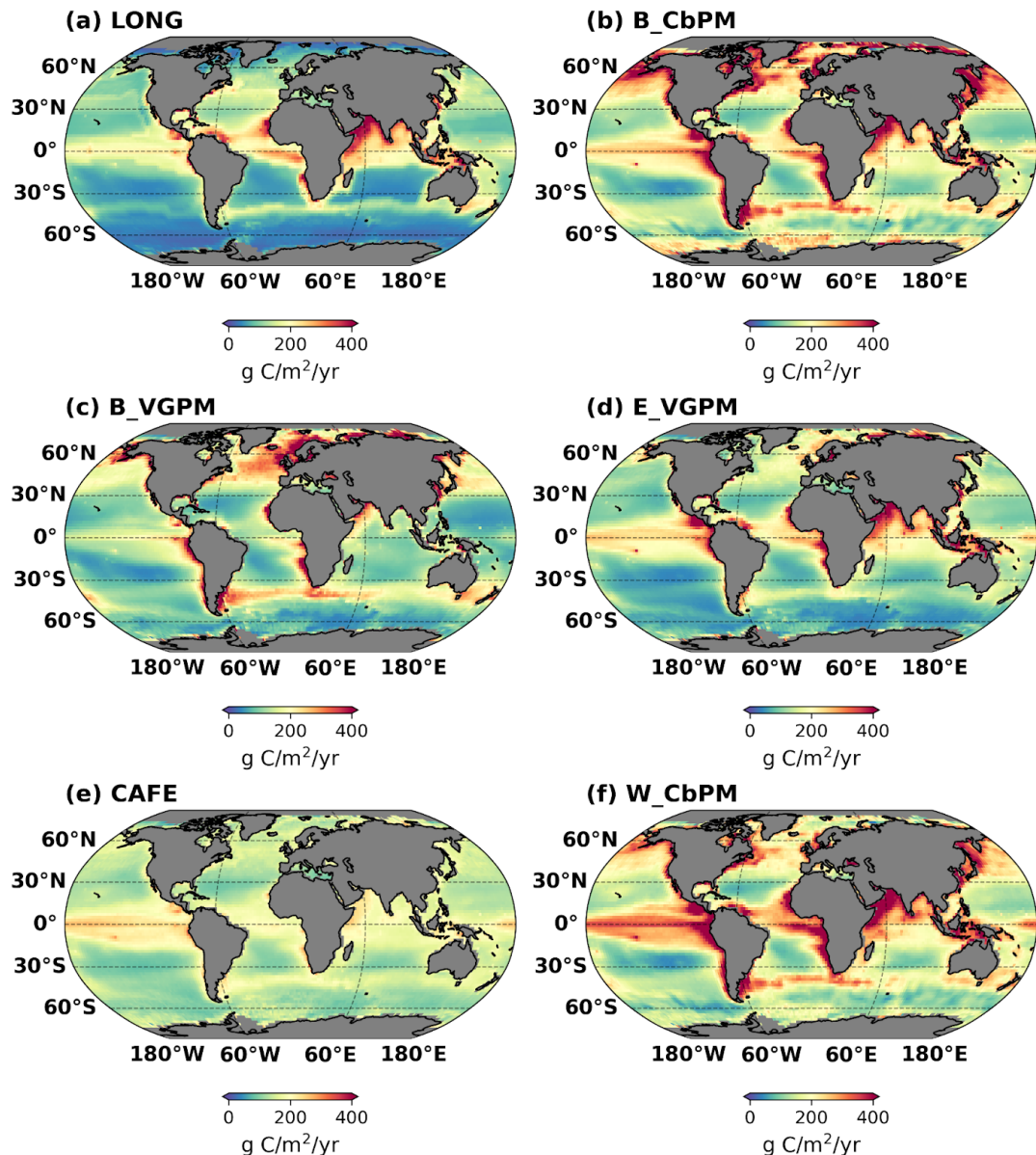
29 References

30 31 S1 Regional Carbon Cycle Assessment and Processes (RECCAP2) biomes



36 S2 Different remote-sensing NPP algorithms

37
38
39
40
41

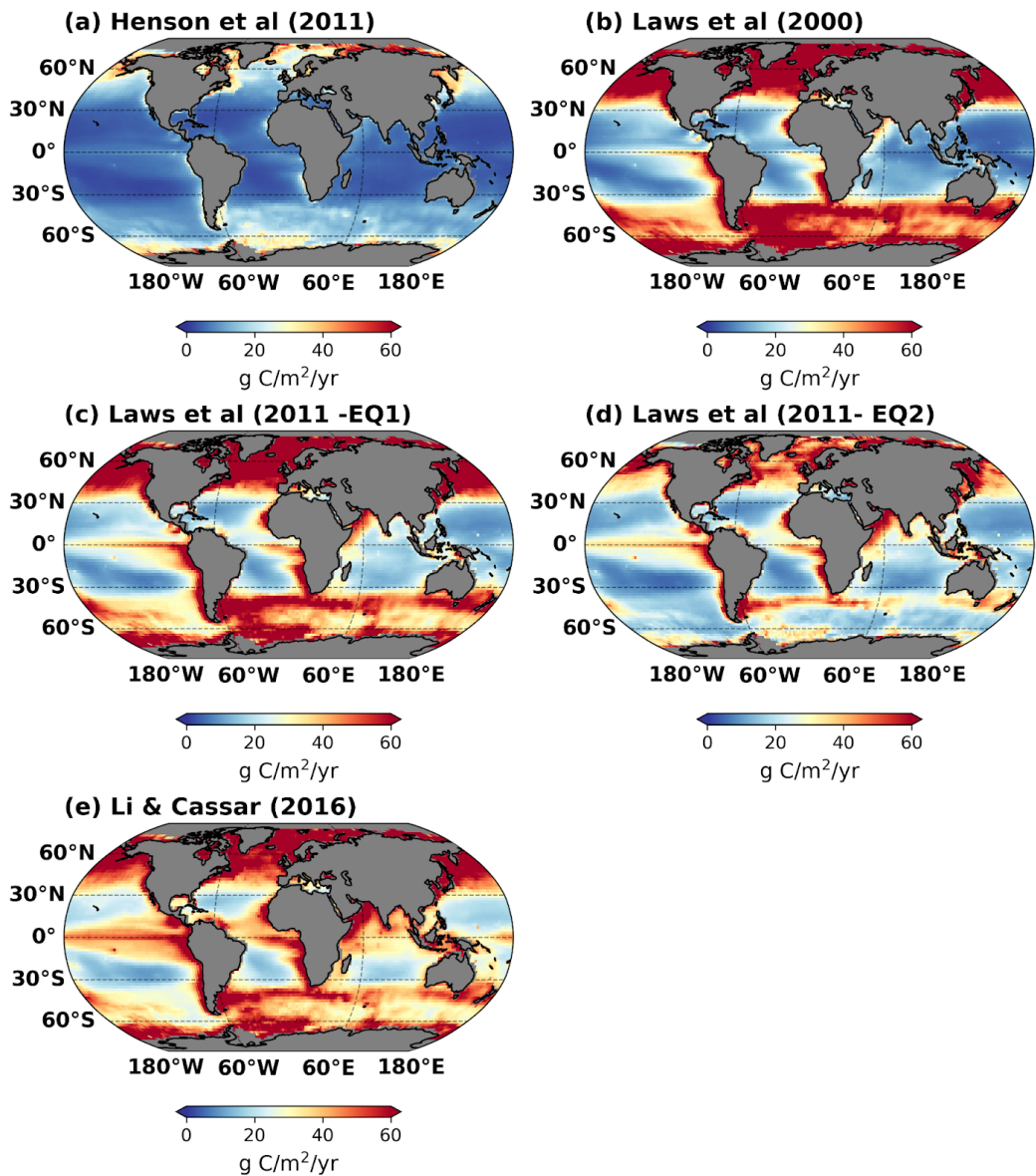


42
43 Figure S2: Mean (1998-2005) of different NPP algorithms.

44
45
46
47
48
49
50
51
52
53

54 S3 Different remote-sensing export production algorithms

55
56
57
58



59

60 Figure S3: Mean (1998-2005) of different export production algorithms

61
62
63
64
65
66
67
68
69
70
71
72
73

74 **S4 Export production equations and references**

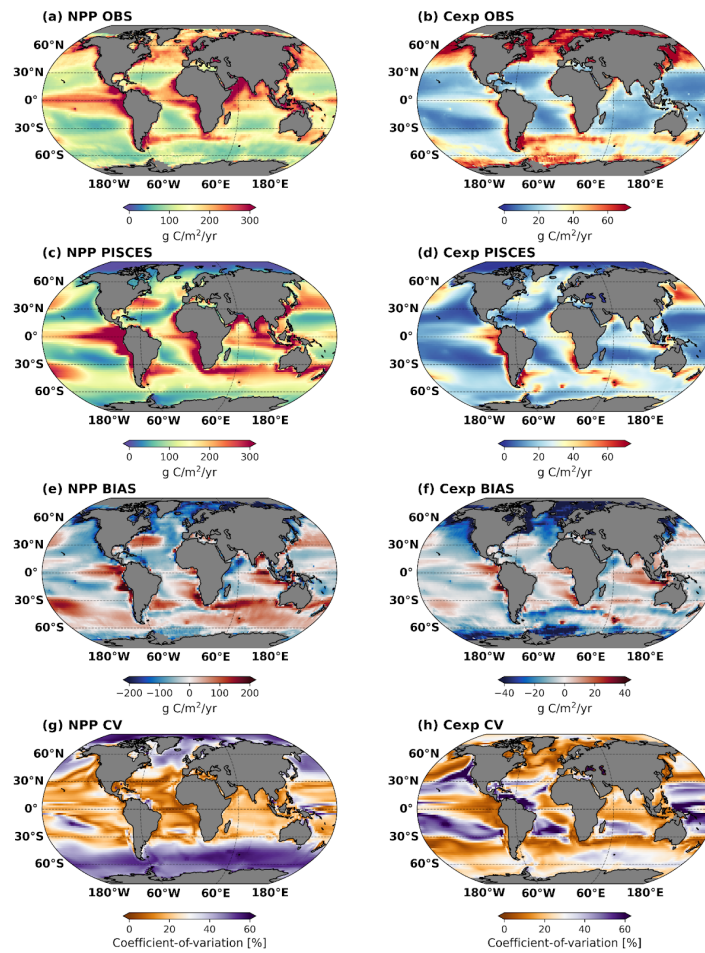
75

76 Table S1: Summary of equations used to compute export production (EP). Both NPP and EP are expressed
 77 in units of $\text{mg C m}^{-2} \text{ day}^{-1}$ and sea surface temperature (SST) in $^{\circ}\text{C}$. The equations are written as they are
 78 shown in Jönsson et al. (2023).

79

80 Reference	81 Equation
82 Laws et al. (2000)	$EP = NPP \cdot (0.62 - 0.02 SST)$
83 Henson et al. (2011)	$EP = NPP \cdot 0.23e^{-0.08 SST}$
85 Laws et al. (2011) - Eq. 86 (1)	$EP = NPP \cdot \frac{(0.5857 - 0.0165 SST) \cdot NPP}{51.7 + NPP}$
87 Laws et al. (2011) - Eq. 88 (2)	$EP = NPP \cdot 0.04756(0.78 - \frac{0.43 SST}{30}) \cdot NPP^{0.307}$
90 Li and Cassar (2016)	$EP = \frac{8.57 \cdot NPP}{17.9 + SST}$

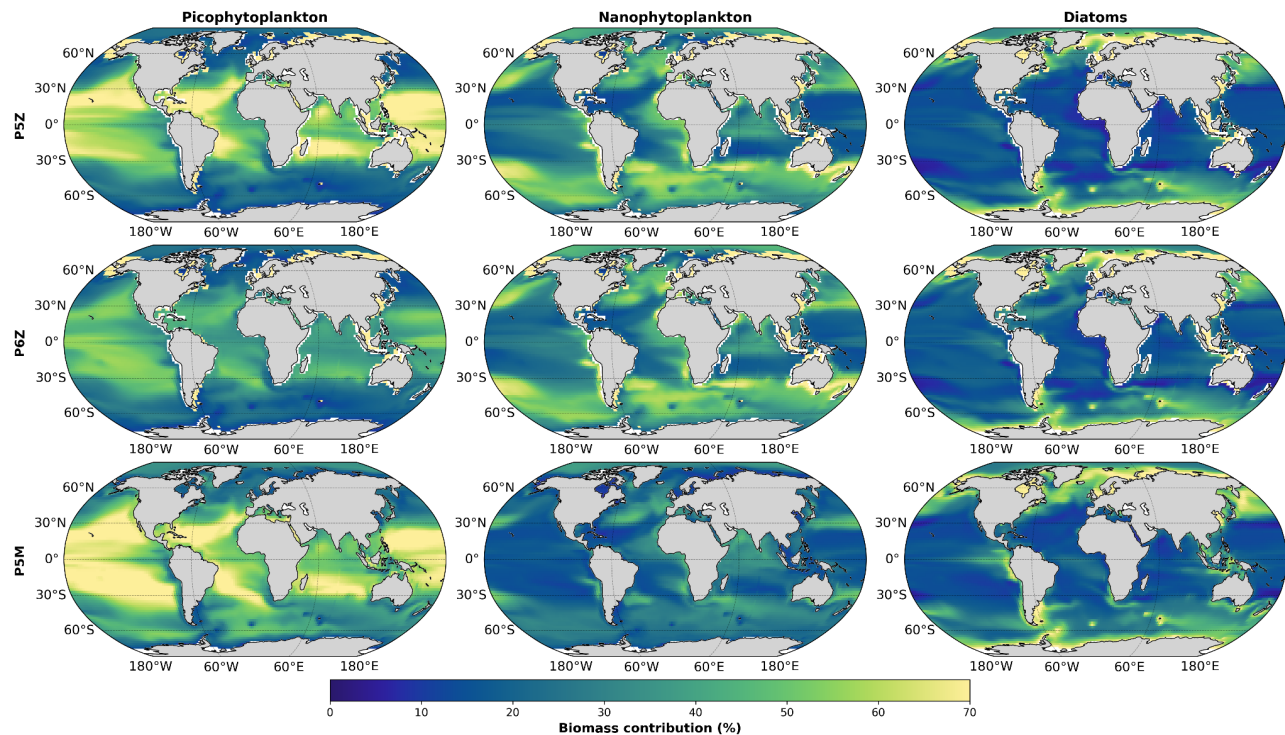
92 **S5 Ensemble mean NPP and C_{exp} of PISCES and remote-sensing**



122 Figure S4: Global maps of satellite derived (a, b) and ensemble model mean (c, d) NPP and C_{exp} . Panels (e)
 123 and (f) show the multi-model mean minus remote-sensing bias while (g) and (h) are the coefficient of
 124 variation (CV) for model NPP and C_{exp} , respectively.

125 **S6 Phytoplankton biomass percentage contribution in Quota-based configurations**

126



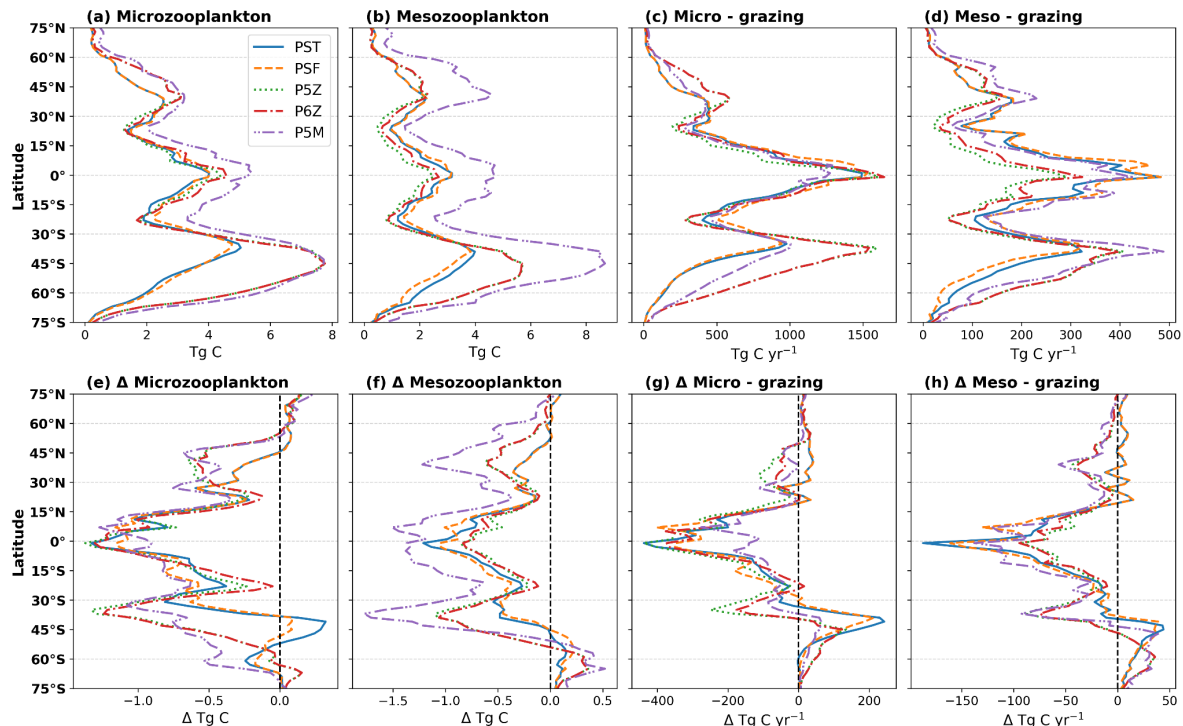
127

128 Figure S5: Percentage mass contribution of pico-, nano, and diatoms to total phytoplankton for the reference
 129 period for the three Quota-based configurations. Note that P6Z shows lower picophytoplankton biomass
 130 because part of the small phytoplankton biomass is allocated to the diazotroph PFT (not shown).

131

132 **S7 Zooplankton dynamics**

133

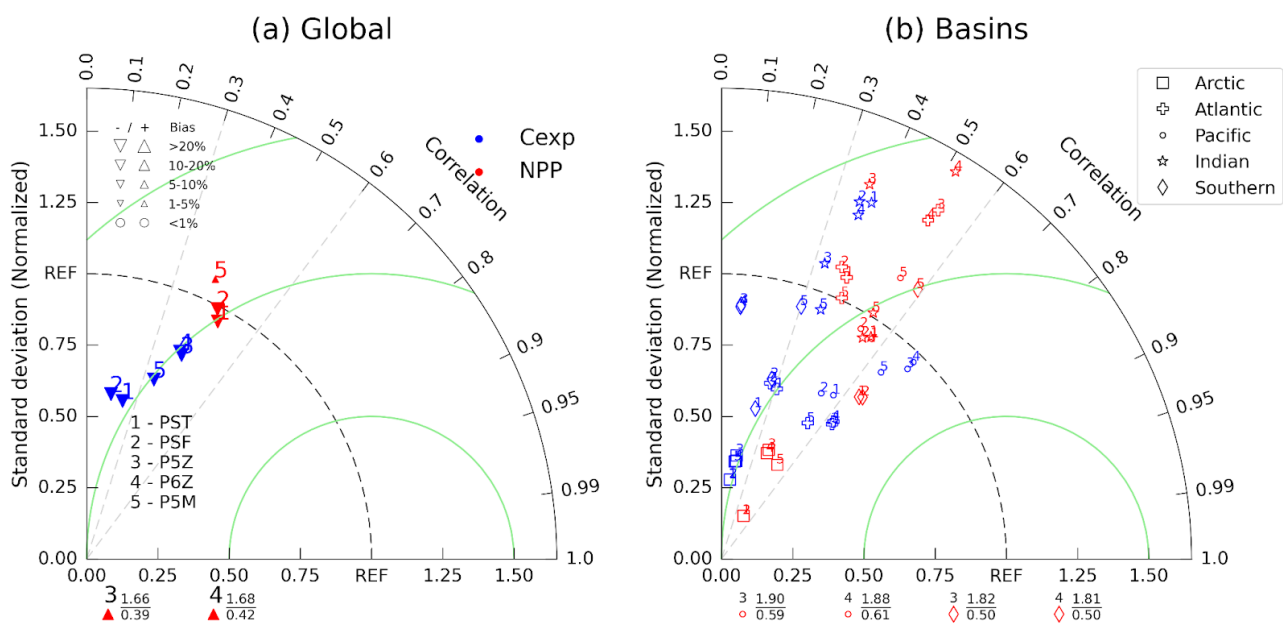


134

135 Figure S6: Top row shows zonally integrated (a) micro- and (b) mesozooplankton biomass along with the
 136 respective grazing rates over the top 100 m. Bottom row (e-h) shows the future shifts

137 **S8** Skill assessment of PISCES configurations versus ensemble mean of remote-sensing
 138 NPP and C_{exp} .

139



140

141

142 Figure S7: Taylor diagrams (Taylor, 2001) showing the (a) global and (b) basin wide performance of the
 143 PISCES configurations compared to remote-sensing. Radial distance represents the ratio of simulated to
 144 remote-sensing standard deviation and azimuthal angle is the model-data correlation. Green arcs show
 145 centered root mean square error between the model and remote-sensing estimates. In (a) and (b), numbers
 146 indicate the PISCES configuration while red and blue points correspond to NPP and C_{exp} , respectively.
 147 Outlier points are shown beneath the respective panels. Top numbers are the standard deviation and lower
 148 values are the correlation coefficient.

149

150 **References**

151

152 Fay, A.R., and McKinley, G.A.: Global open-ocean biomes: mean and temporal variability, *Earth Syst. Sci. Data*, 6(2),
 153 273-284, <https://doi.org/10.5194/essd-6-273-2014>, 2014.

154

155 Jönsson, B.F., Kulk, G., and Sathyendranath, S.: Review of algorithms estimating export production from satellite
 156 derived properties, *Front. Mar. Sci.*, 10, 1149938, <https://doi.org/10.3389/fmars.2023.1149938>, 2023.

157

158 Taylor, K.E.: Summarizing multiple aspects of model performance in a single diagram, *J. Geophys. Res-Atmos.*,
 159 106(D7), 7183-7192, <https://doi.org/10.1029/2000JD900719>, 2001.

160

161

162